water

MDPI

Article

Evaluating the Hydrological Impact of Reservoir Operation on Downstream Flow of Seomjin River Basin: SWAT Model Approach

Hiyaw Hatiya Ware [1,2], Sun Woo Chang [1,2], Jeong Eun Lee [2,*] and Il-Moon Chung [1,2,*]

[1] Civil and Environmental Engineering Department, University of Science and Technology (UST), Daejeon 34113, Republic of Korea; hhiyaw1990@kict.re.kr (H.H.W.); chang@kict.re.kr (S.W.C.)
[2] Department of Water Resources and River Research, Korea Institute of Civil Engineering and Building Technology, Goyang 10223, Republic of Korea
* Correspondence: jeus22@kict.re.kr (J.E.L.); imchung@kict.re.kr (I.-M.C.)

Abstract: Multi-purpose dams in a river basin frequently result in variations in downstream flow. Precisely assessing the reservoir operation effects can improve management strategies and alleviate extreme hydrological events. This study assesses the impact of reservoir operation scenarios on the downstream flow in the Seomjin River basin in South Korea. Four reservoir scenarios were developed utilizing observed daily inflow and outflow data from the reservoirs. A semi-disturbed hydrological model, SWAT (Soil and Water Assessment Tool), was employed to simulate the flow for each reservoir operation scenario in the downstream section of the study basin. Model execution was evaluated by comparing the simulated and measured streamflows using performance metrics, including R^2, NSE, and PIBAS, which displayed very good compatibility. The sensitivity of calibration parameters varied across different reservoir operation scenarios. The results of this study indicate that the operation scenarios for the Seomjin and Juam reservoirs led to a maximum downstream flow reduction of 32%. Additionally, the monsoon season exhibited a lower percentage reduction in flow compared to the dry season, which was influenced by the frequency of rainfall in the region. Annual assessment indicated that streamflow reduction varies between 1.35% and 32.9% across all reservoir operation scenarios. Reservoir operations have demonstrated their effect on the alteration of downstream flow in the Seomjin River basin. This study demonstrates that the operation of the Seomjin reservoir has a more significant impact on downstream flow than that of the Juam reservoir in the study region. This study analyzed a substantial basin with various reservoir operation scenarios to assess the influence of flow on the downstream section, yielding important insights for efficient water resource management.

Keywords: SWAT; reservoir routing; streamflow; reservoir scenario

Citation: Ware, H.H.; Chang, S.W.; Lee, J.E.; Chung, I.-M. Evaluating the Hydrological Impact of Reservoir Operation on Downstream Flow of Seomjin River Basin: SWAT Model Approach. *Water* **2024**, *16*, 3584. https://doi.org/10.3390/w16243584

Academic Editor: Alexander Shiklomanov

Received: 30 October 2024
Revised: 21 November 2024
Accepted: 7 December 2024
Published: 12 December 2024

1. Introduction

Streamflow is a fundamental component of the hydrological system and a crucial resource for the ecosystem of human development [1,2]. Various factors influence streamflow, which can be categorized as climatic or resulting from human activities [3,4]. Climate factors influence the streamflow by altering its spatial and temporal distribution and include precipitation, temperature, and evaporation. Meanwhile, human activities affect streamflow processes and routing by modifying land use/land cover and constructing water management structures such as reservoirs and dams [5,6]. The streamflow condition in a basin is an essential indicator of climatic and environmental alterations. Thus, understanding and accurately estimating streamflow are crucial for drought monitoring, reservoir management, flood forecasting, water quality assessment, and overall water resource management [7–9]. Despite advanced methods, precise streamflow estimation remains challenging because of the intricate interaction between climate and human influences on the basin hydrological cycle response [10,11].

Hydrological structures, such as dams and reservoirs, deliver considerable advantages to human societies by boosting water accessibility for urban, industrial, and farming needs. Reservoirs play a vital role in flood control by moderating the effect of potentially devastating floods and generating hydropower, which provides a renewable and reliable source of electricity [12,13]. However, reservoir operation can have dual effects on a hydrological watershed. On the positive side, these structures effectively manage flow regimes by adjusting the spatiotemporal variations in river flow, which is particularly beneficial for mitigating hydrological extremes such as floods and droughts [14–16]. Previous research suggests that reservoirs can alleviate hydrological drought in downstream regions by discharging stored water during dry periods or promoting groundwater recharge, which restores the baseflow component of river streams [17–19]. On the other hand, reservoirs can negatively affect downstream areas by increasing evaporation, disrupting floodplain hydrological processes, altering the spatial and temporal patterns of streamflow hydrographs, fragmenting river ecosystems, and leading to the deterioration of natural river valleys [20–22]. Some studies have proven that over-reliance on reservoirs can lead to potential drought to some extent due to water supply demand [23,24]. Therefore, utilizing proper hydrological models with available data could benefit users in evaluating the impacts of reservoirs on the downstream hydrological regimes.

In South Korea, more than 20 multi-purpose dams play a dynamic part in supporting socio-economic development and promoting environmental sustainability. The hydrological structures manage floods and droughts during the monsoon and dry seasons. At times, extreme events may influence their operation, requiring the retention or release of significant water volumes, which can alter the downstream hydrological regime [25,26]. The Seomjin River basin, located in the central western area of the South Korean southern coast, is home to two major multi-purpose dams. These dams serve various functions, including water supply, flood control, industrial use, hydropower generation, and maintaining environmental flow. In August 2020, the basin was hit by an unprecedented extreme flood event that resulted in the loss of life and severe infrastructure damage. Such extreme events underscore the need to evaluate the impacts of reservoir operations on downstream flow within the watershed. Thus, understanding the intricate relations among reservoir operations and hydrological processes is crucial for improved water resource and ecological management.

Modeling is the most widely used approach for studying and quantifying the impacts of hydrological structures in the watershed. Hydrological models provide an alternative to simulate scenarios of reservoir operation and visualize various stream locations as a whole or separately [27]. Further, the hydrological models can analyze the combination of water transfer and reservoir operation in a study basin. Several studies have adapted hydrological models to evaluate the streamflow of basins and demonstrated the strong ability of models to simulate the existing scenarios of basins. However, some models do not fully incorporate basin reservoir operation, water transfer, and hydrological water components [27–29]. Models such as HEC-ResSim are mainly used for reservoir analysis, which requires linkage with other numerical models to assess the impact on basin flow regimes [25]. The Soil and Water Assessment Tool (SWAT) is a semi-distributed watershed model that is highly effective for managing water resources and watershed applications at a watershed scale. This model offers multiple features with various applications, resulting in high flexibility and adaptability for adjusting hydrological components under different conditions. The precision of hydrological model simulations rests on the input data provided by the users to represent local or regional target basins. Excluding reservoir routing in hydrological modeling processes impacts watershed streamflow simulations [30,31].

Researchers frequently investigate hydrological extremes at local and regional levels under the assumption of natural flow conditions, even though watersheds downstream flow in a worldwide pattern and are regulated by reservoir operation. This practice overlooks the significant influence that reservoir regulation can have on drought and flood dynamics [32,33]. Other studies demonstrate that the presence of a reservoir significantly

impacts water resource allocation, in addition to flood and drought prevention in the basin [34–36]. Therefore, acquiring accurate information about reservoirs is essential as a vital input for hydrological model simulations.

Models incorporating reservoir routing have demonstrated a robust influence on flow regimes, temporal flow distribution, and hydrological extreme events [18,37,38]. The reservoir module includes a water balance specific to the existing reservoir within the designated subbasin. Further, the model offers four different methods for estimating reservoir outflow: daily outflow, monthly outflow, average annual outflow for uncontrolled reservoirs, and target releases for controlled reservoir measurements [39]. The daily outflow estimation approach was employed in this paper, utilizing 20 years of daily-observed inflow and outflow data from the existing dams. Furthermore, scenarios were created to evaluate the impact of reservoir operations on the downstream flow, by utilizing the inflow and outflow information for the study region.

The Seomjin River basin was selected as a case study region to analyze the effects of reservoir operation on the downstream flow. The objectives of this study are (i) to assess the impact of reservoir inflow and outflow on the downstream flow conditions; (ii) to evaluate the effects of individual and combined reservoir flow on the downstream flow of the basin; and (iii) to weigh the parameter sensitivity towards the reservoir scenario of the study watershed. This study provides valuable insight into the simulation of reservoir routing using the SWAT model with daily-recorded reservoir inflow and outflow values. Further, this study highlights the water balance of the Seomjin watershed.

2. Materials and Methods

2.1. Description of Study Area

The Seomjin River basin, one of South Korea's five major rivers, is located in the southwestern region of the country. The Nakdong River Basin borders the basin to the east and the Geum and Mangyeon River basins to the north. The study basin covers an area of 4611.52 square kilometers, with a main river channel length of 223.86 km (see Figure 1). Known for its exceptional ecological value, the Seomjin River supports diverse aquatic life, including fish and shellfish, and is recognized for its pristine water quality and scenic landscape. The basin experiences an average annual rainfall of 1432.6 mm, which is higher than the national average of 1278 mm, with most precipitation occurring during the summer monsoon season (July–September). The Seomjin River basin features varying topography, with elevations reaching up to 1537.2 m and an average height of 306 m above sea level. A significant portion of the basin (45.5%) has slopes exceeding 35%, contributing to its unique hydrological and ecological characteristics. This geographic and climatic diversity makes the Seomjin River basin an essential area for studying hydrology, ecology, and sustainable water resource management.

The Seomjin River basin houses two major multi-purpose dams, Seomjin and Juam, which are critical for regional water resource management and power generation. The Seomjin Dam, a concrete gravity structure located in the northeastern part of the basin, stands 64 m high with a crest length of 344.2 m. It has an overall storage capacity of 466 million cubic meters (m^3) and supplies 435 million m^3 of water annually, with an installed hydropower capacity of 34.8 megawatts (MW). In contrast, Juam Dam, an earth-core rockfill dam, measures 58 m in height with a crest length of 330 m, offering an effective storage capacity of 352 million m^3 and a total capacity of 457 million m^3. Juam Dam supplies 271 million m^3 of water annually and generates 1.4 MW of electricity. Both dams play essential roles in water supply, electricity generation, and flood control for the region, contributing significantly to the hydrological balance and resource sustainability of the Seomjin River basin. Table 1 presents the detailed characteristics of the Seomjin and Juam reservoirs.

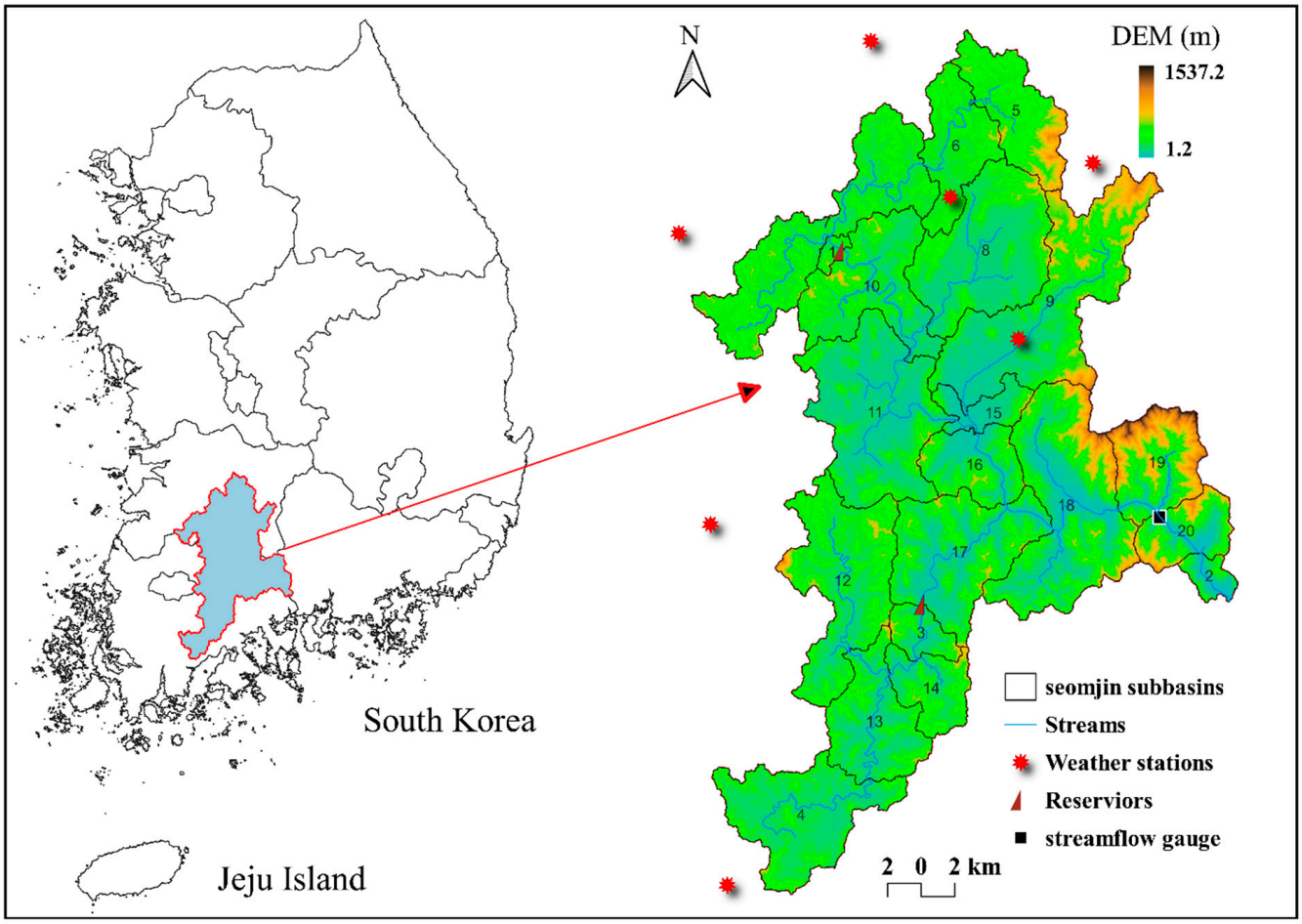

Figure 1. Seomjin River basin including reservoirs, weather stations, streamflow gauge, and Digital Elevation Model (DEM).

Table 1. Description of the two multi-purpose dams in the Seomjin River basin.

Reservoir Parameters Used During SWAT Simulation												
Parameter	**Description**										**Value**	
											Seomjin Dam	**Juam Dam**
RES_ESA	Reservoir surface area when the reservoir is filled to emergency spillway (ha)										2425	3000
RES_EVOL	Volume of water needed to fill the reservoir to the emergency spillway (104 m^3)										46,600	45,700
RES_PSA	Reservoir surface area when the reservoir is filled to the principal spillway (ha)										2312	2880
RES_PVOL	Volume of water needed to fill the reservoir to the principal spillway (104 m^3)										40,000	40,330
RES_VOL	Initial reservoir volume (104 m^3)										25,120.6	23,546
RES_K	Hydraulic conductivity of the reservoir bottom (mm/hr)										0.5	0.5
EVRSV	Lake evaporation coefficient										0.6	0.6
	Monthly Data for Seomjin Dam											
WURESN	Average daily water withdrawn from reservoir each day in the month for consumptive use (10^4 m^3)											
Month	1	2	3	4	5	6	7	8	9	10	11	12
Value	24.1	31.2	44.6	123.4	253.6	258.3	199.5	238.8	207.5	66.8	27.4	21.0
	Monthly Data for Juam Dam											
WURESN	Average daily water withdrawn from reservoir each day in the month for consumptive use (10^4 m^3)											
Month	1	2	3	4	5	6	7	8	9	10	11	12
Value	72.9	77	82.5	87.1	104.3	121.8	156.8	159.3	144.5	121.2	100.1	80.2

Figure 2 illustrates the distribution of hydrological soil groups within the Seomjin River basin, revealing that soil group "D", characterized by low infiltration and high surface

runoff potential, is the most prevalent, covering 45.6% of the watershed. Group "C" is the least common, occupying only 1.5%, while groups "A" and "B" cover 25.8% and 27.1%, respectively. Figure 3 presents the land use and land cover (LULC) classification for the Seomjin watershed, showing forestland as the dominant type, accounting for 70% of the area, followed by rice paddies at 14%, and urban land at less than 3%.

The public websites (http://www.naas.go.kr/ accessed on 20 November 2024) and (https://egis.me.go.kr/intro/land.do accessed on 20 November 2024) were the source of the study basin soil and LULC maps, respectively. The weather and streamflow information were accessed from (https://data.kma.go.kr/cmmn/main.do accessed on 20 November 2024) and (http://www.wamis.go.kr/ accessed on 20 November 2024), respectively, which are public platforms. Further, the inflow and outflow data for the reservoirs in the study watershed were sourced from (https://www.water.or.kr accessed on 20 November 2024), a public governmental agency website.

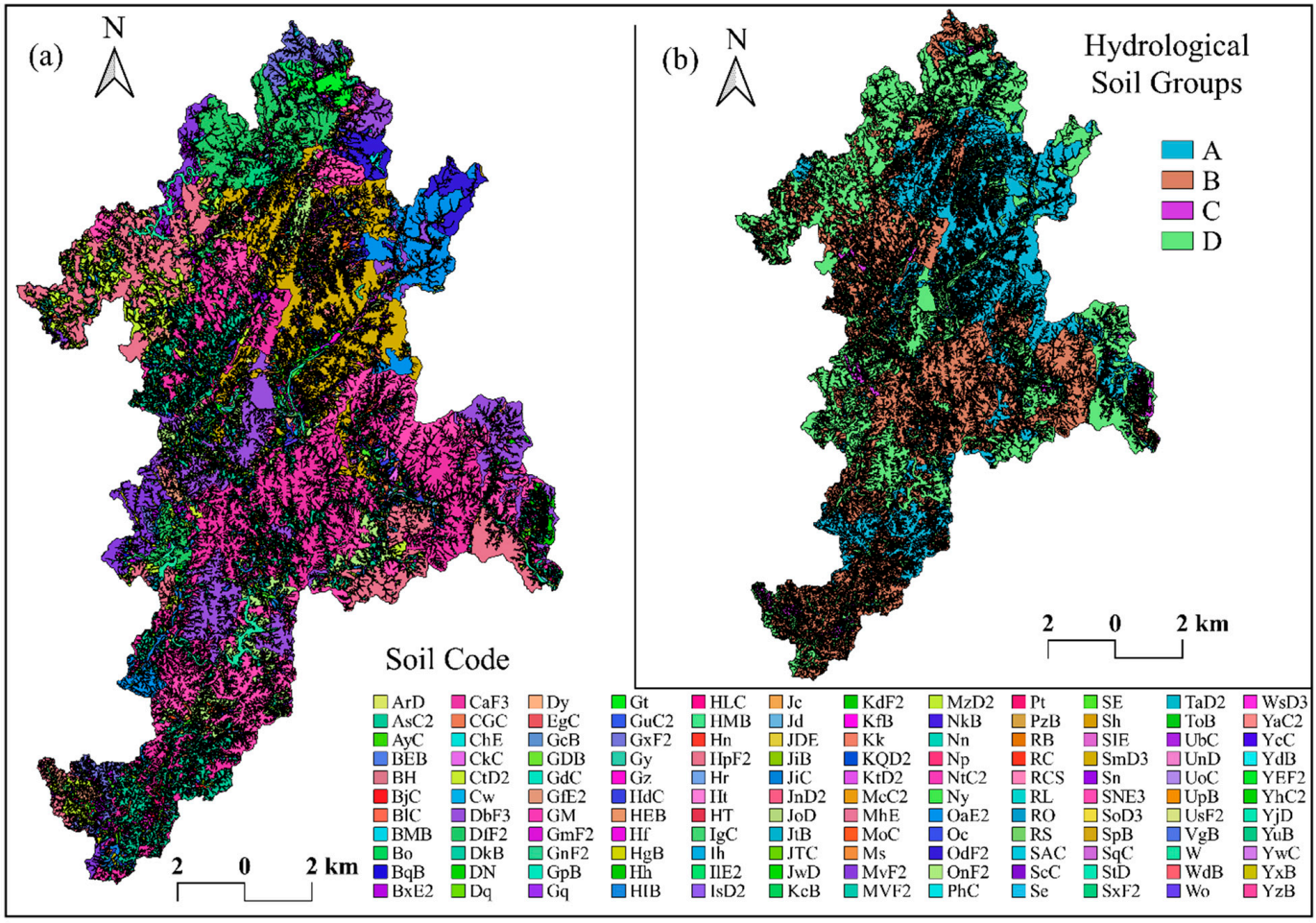

Figure 2. Study region soil classification: (**a**) soil code and (**b**) hydrological group.

Figure 4 presents the flowchart used to estimate the influence of reservoir operations on the downstream flow of the Seomjin River basin. The following reservoir scenarios were established: (S1) both Seomjin and Juam dams operating, (S2) no dams operating, (S3) only the Seomjin dam operating, and (S4) only the Juam dam operating. The outflow from subbasin 2 (see Figure 1) was selected to represent the downstream flow. After model calibration, the streamflow from subbasin number 2 was utilized to assess the impact of these scenarios. For scenarios with reservoir operations (S1, S3, and S4), the observed outflow data were incorporated into the model database, while for the scenario without dam operations (S2), the recorded inflow was employed. Additionally, the average daily

water withdrawals, as detailed in Table 1, were included in the monthly model, according to the reservoir operation scenario.

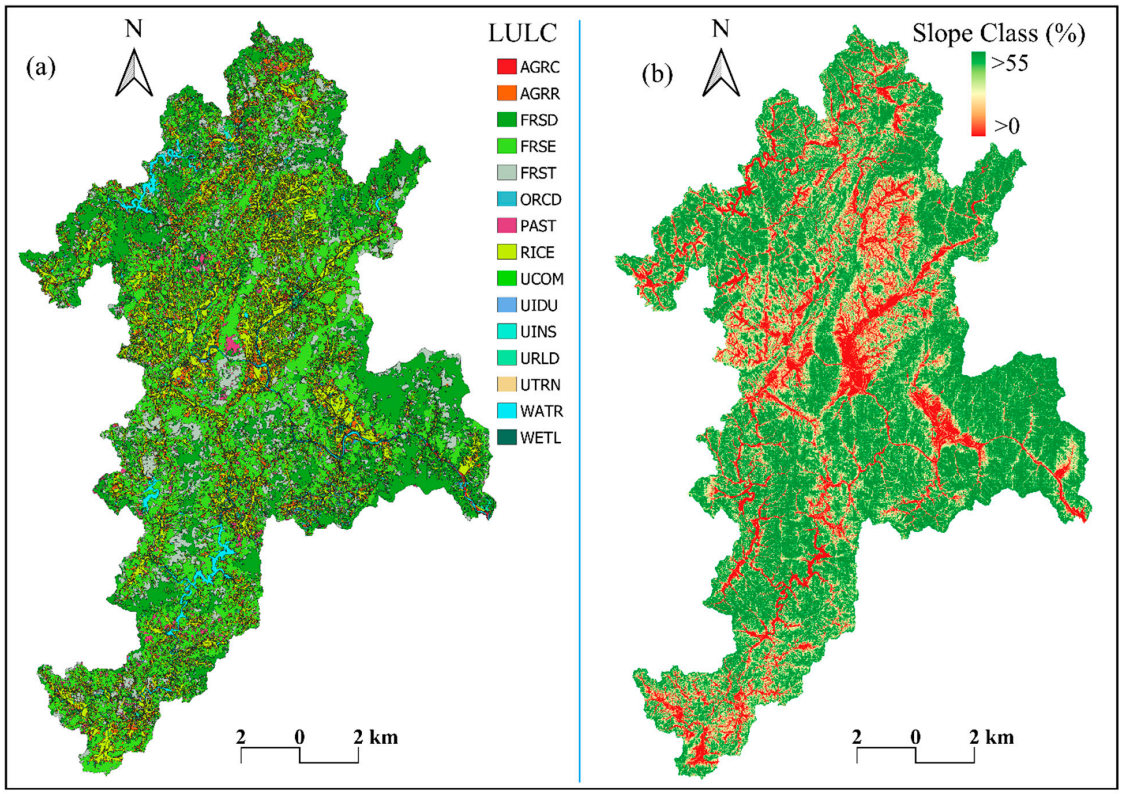

Figure 3. Seomjin watershed: (**a**) land use and land cover (LULC) classification and (**b**) slope class.

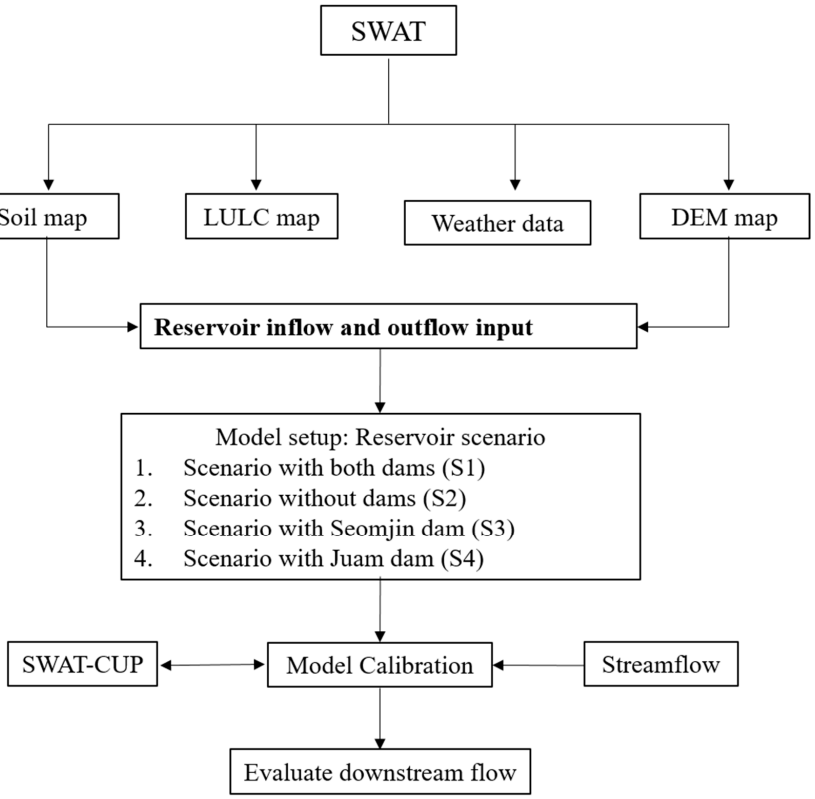

Figure 4. Flowchart: overview approach utilized for current study.

2.2. SWAT Model and Module for Reservoir

SWAT is one of the most widely recognized open-source, semi-distributed, and continuous daily time-step hydrological models and is employed to assess the effects of land use, climate change, and various management practices on water flow, sediment transport, and agricultural chemical yields in a watershed over a specified period [40,41]. The SWAT framework divides a watershed into subbasins, which are further segmented into hydrological response units (HRUs). A unique combination of LULC, soil type, slope, and management practices defines each HRU. The SWAT model uses a water balance Equation (1) to simulate hydrological processes, allowing for the detailed evaluation of the interactions between the hydrological water components.

$$SWt = SWo + \sum_{t=1}^{t} \left(R - Q_{sur} - ET - Q_{perc} - Q_{gw}\right) \quad (1)$$

In SWAT modeling, reservoirs are key water bodies positioned along the main channel network of a watershed, where they gather inflows from upstream subbasins. These reservoirs are strategically located to regulate downstream hydrology by controlling the flow, sediment, and nutrient loads. Thus, reservoirs are crucial in shaping the hydrological and water quality dynamics of watersheds. Equation (2) governs the water balance of the SWAT reservoir model.

$$V = V_{stored} + V_{flowin} - V_{flowout} + V_{pcp} - V_{evap} - V_{seep} \quad (2)$$

where V denotes the amount of water in reservoir at the end of the day, V_{stored} is the initial water stored at the start of the day, V_{flowin} is the amount of water entering the reservoir during the day, $V_{flowout}$ is the amount of water volume exiting the reservoir during the day, V_{pcp} is the rainfall amount falling on the reservoir during the day, V_{evap} is the water lost through evaporation from the reservoir during the day, and V_{seep} is the amount of water lost from the reservoir by seepage. All of the stated variables are in cubic meters (m^3). The V_{pcp}, V_{evap}, and V_{seep} are each estimated as a function of the daily water surface of the reservoir [41].

In SWAT modeling, the volume of water released from the reservoir ($V_{flowout}$) can be determined through four different approaches:

1. Using recorded daily outflow rates;
2. Using measured monthly outflow rates;
3. Applying a mean yearly release rate for reservoirs without flow control mechanisms;
4. Utilizing a target release rate for reservoirs with controlled outflows.

When the measured daily outflow approach is used, the reservoir inflow and outflow are calculated including the data provided by the user as daily discharge data during the simulation. This study employs the measured daily outflow method since it enhances the reliability of hydrological simulation. Detailed information on the reservoir component in SWAT is available in [41].

Figure 5 illustrates the daily-observed inflow and outflow values for the Seomjin and Juam reservoirs in the basin. Figure 5a displays the downstream flow from these reservoirs to the lower subbasins of the basin. The maximum daily-observed outflow from the Seomjin reservoir was 1356 m^3/sec in August 2020, while in Juam, the highest outflow of 1146.7 m^3/sec occurred in September 2007. The peak daily inflow was 1716.2 m^3/sec for Juam and 2000.9 m^3/sec for Seomjin, observed during the extreme event in the study basin. The average monthly inflow was 19.05 m^3/sec for Seomjin and 22.3 m^3/sec for Juam, with peak inflows observed in July and August, respectively. The average monthly outflow was 4.6 m^3/sec for Seomjin and 9.6 m^3/sec for Juam, with August displaying the highest average outflow for both reservoirs.

The inflow and outflow data from Figure 5 were utilized to develop reservoir operation scenarios and assess their impact on the downstream section of the study basin. The

reservoir characteristics from Table 1 were also integrated into the SWAT model, following the operation scenario outlined in Figure 4.

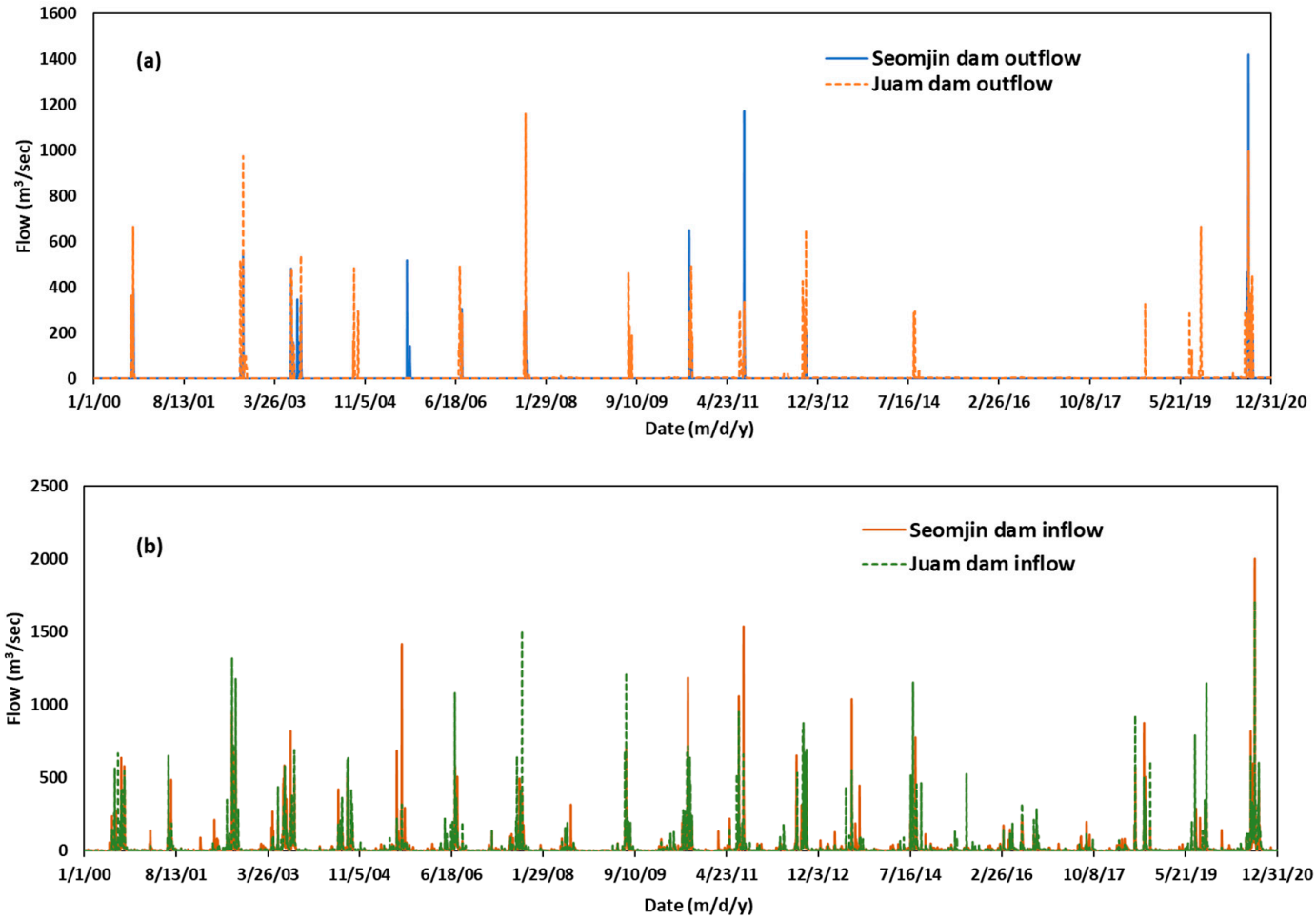

Figure 5. Seomjin and Juam reservoirs: (**a**) outflow values and (**b**) inflow values.

2.3. Model Setup and Calibration Process

The SWAT model (version 636) was employed to simulate the hydrological dynamics of the Seomjin River basin, dividing it into 20 subbasins and 1627 hydrological response units (HRUs) based on factors such as the slope, soil type, land use, outlets, and reservoir locations. In this study, for each scenario shown in Figure 4, a distinct SWAT model database was developed. Calibration and validation utilized the SWAT-CUP tool with the SUFI-2 algorithm, assessing model performance through the correlation coefficient (R^2), Nash–Sutcliffe Efficiency (NSE), and percent bias (PBIAS). The model simulation spanned 1998 to 2020, including a two-year warm-up, with calibration from 2008–2015 and validation from 2016–2020 on a daily time step to align with the reservoir input data.

This study selected sixteen parameters to calibrate the initial SWAT model, as stated in Table 2. The SWAT-CUP tool was used to categorize sensitive parameters with the values of the sensitivity indices (p and t). Manning's value for the main channel (CH-N2) was recognized as the most sensitive parameter, followed by the slope length of lateral subsurface flow (SLSOIL) in all reservoir model scenarios. The sensitivity rankings varied after the first and second ranks, depending on the reservoir scenario. For instance, the curve number ranked third for scenarios 1 and 2 of the basin. However, for individual reservoir operations, the Manning's value for the overland flow (OV_N) parameter ranked third.

Table 2. Selected parameters for the SWAT model in the Seomjin River basin.

Calibration Parameter	Description	Calibrated Range Value	Fitted Value
r__CN2.mgt	Initial SCS runoff curve no. for moisture condition II	−0.5–0.2	−0.45
v__CH_N2.rte	Manning's "n" value for main channel	0.06–0.3	0.07
v__ALPHA_BF.gw	Baseflow alpha factor (days)	0–1	0.09
v__GW_DELAY.gw	Groundwater delay (days)	1–5	1
v__GWQMN.gw	Threshold depth of water in the shallow aquifer required for return flow to occur (mm)	0–2000	1058
v__GW_REVAP.gw	Groundwater "revap" coefficient	0.02–0.2	0.026
v__ESCO.hru	Soil evaporation compensation factor (-)	0.01–1	0.42
v__EPCO.hru	Plant uptake compensation factor (-)	0–1	0.91
r__SOL_AWC().sol	Available water capacity of the soil layer (mm mm^{-1})	−0.4–0.2	0.12
v__RCHRG_DP.gw	Deep aquifer percolation fraction	0–1	0.68
v__CANMX.hru	Maximum canopy storage	0–10	1.67
v__SLSOIL.hru	Slope length of lateral subsurface flow (m)	0–10	3.97
v__REVAPMN.gw	Threshold depth of water in the shallow aquifer for "revap" to occur (mm)	0–500	86.5
r__HRU_SLP.hru	Average slope steepness (m/m)	−0.1–0.1	0.076
r__OV_N.hru	Manning's "n" value for overland flow	−0.1–0.1	−0.037
v__SURLAG.bsn	Surface runoff lag coefficient	0–7	0.71

The calibrated range values used in the SWAT-CUP for each reservoir scenario were the same as in Table 2. However, the fitted values of selected parameters were different concerning reservoir scenarios. The fitted values illustrated in Table 2 are for scenario 1. To estimate the reliability of the simulation results produced by the SWAT model, we utilized the Nash–Sutcliffe Efficiency (NSE) as the objective function. The NSE measures the model's overall efficiency, with higher NSE values indicating greater reliability of the simulated outcomes. Additionally, the coefficient of determination (R^2) was employed to assess the degree of correlation between the simulated and measured data; a higher R^2 value signifies a more substantial similarity in the trend between the two datasets. The percent bias (PBIAS) was used to quantify the deviation of the simulated data from the observed data's average trend. Specifically, a negative PBIAS indicates model overestimation, a positive PBIAS indicates underestimation, and a PBIAS of zero reflects a perfect agreement between the simulated and observed values. Detailed descriptions and classifications of these performance indicators are available in Moriasi et al., 2007 [42]. The respective calculations for these indicators can be performed using the following equations.

$$R^2 = \frac{\left[\sum_{i=1}^{n}\left(Q_{obs,i} - Q_{mobs}\right) * \left(Q_{sim,i} - Q_{msim}\right)\right]^2}{\sum_{i=1}^{n}\left(Q_{obs,i} - Q_{mobs}\right)^2 * \sum_{i=1}^{n}\left(Q_{sim,i} - Q_{msim}\right)^2} \quad (3)$$

$$NSE = 1 - \frac{\sum_{i=1}^{n}\left(Q_{obs,i} - Q_{sim,i}\right)^2}{\sum_{i=1}^{n}\left(Q_{obs,i} - Q_{mobs}\right)^2} \quad (4)$$

$$PBIAS = \left[\frac{\sum_{i=1}^{n} Q_{obs,i} - \sum_{i=1}^{n} Q_{sim,i}}{\sum_{i=1}^{n} Q_{mobs}}\right] * 100 \quad (5)$$

where $Q_{obs,i}$—measured value, $Q_{sim,i}$—simulated value, Q_{mobs}—mean observed value, and Q_{msim}—mean simulated value.

3. Results

3.1. Model Calibration and Validation

Figure 6 presents the daily simulated and observed streamflow during the calibration and validation period of the study region. The simulated streamflow closely matches

the observed values in both phases, with the SWAT-CUP model accurately capturing the peak values and timing (see Figure 6). Figure 6b,c shows the strong correlation between the observed and simulated streamflows during the calibration and validation phases. Statistical performance indicators can assess the model's performance in simulating the observed streamflow of a study region. Table 3 presents the model performance indicators during the calibration and validation periods. The values specified in Table 3 reveal that the model performed well following the model performance guidelines stated by Moriasi [42].

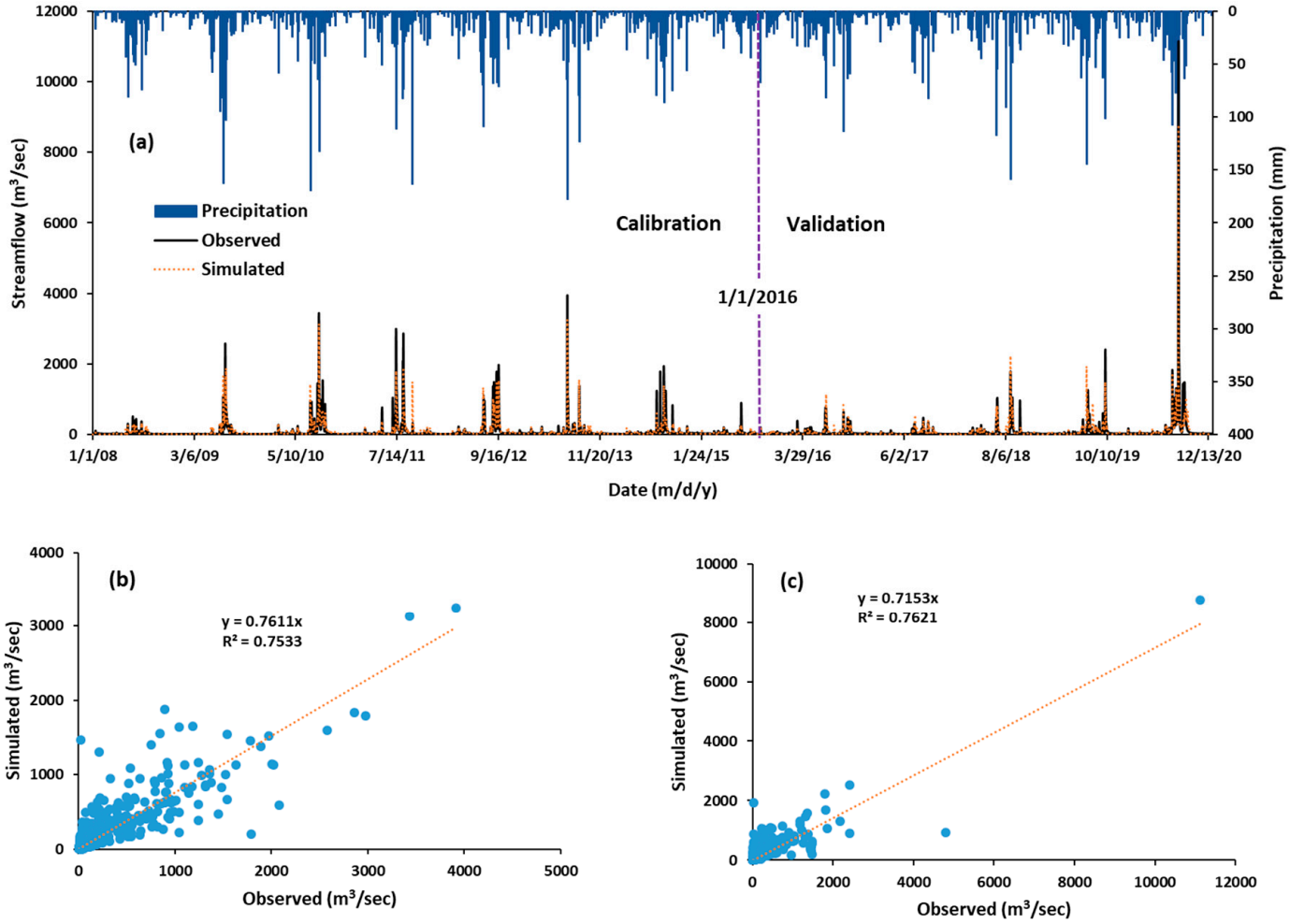

Figure 6. Streamflow: (**a**) observed and simulated vs. time for calibration and validation periods, (**b**) observed vs. simulated during calibration, and (**c**) observed vs. simulated during validation.

Table 3. SWAT model performance indictors during calibration and validation periods.

Station	Calibration (2008–2015)			Validation (2016–2020)		
	R^2	NSE	PBIAS	R^2	NSE	PBIAS
Gwangyangsi	0.77	0.77	−3.0	0.77	0.76	0.8

At the streamflow gauge, these model performance indicators show a good fit between the simulated and observed values, as presented in Table 3. During calibration, the model slightly overestimated the observed streamflow, as reflected by a negative PBIAS, while it underestimated the streamflow during validation for the study watershed. According to the model performance classification by [42], the model was rated as "very good" for the calibration and validation periods. The stated results in this section are solely based

on reservoir operation scenario 1, which accounts for the current situation of the Seomjin River basin.

3.2. The Impact of Reservoir Operation on the Downstream Flow

Reservoir operation significantly impacts the downstream flow rate, magnitude, and fluctuation during the dry and wet seasons of the study watershed [43,44]. Figure 7 displays the monthly and annual average downstream flow patterns for each Seomjin River basin reservoir scenario. South Korea experiences the monsoon season from July to September, which brings heavy rainfall, including in the Seomjin River basin. Figure 7 depicts the seasonal flow variations in the study watershed in all reservoir scenarios. For the monthly downstream hydrograph, the maximum flow happened in August for the reservoir scenarios of the study basin, as displayed in Figure 7a. January exhibited a lower flow magnitude for each reservoir scenario, as shown in Figure 7a. The mean monthly flow value ranged from 93.8–119 m^3/sec for all reservoir scenarios. In October, all reservoir scenarios showed less discrepancy from the mean monthly range values. In the case of individual reservoir operation, that is, scenarios 3 and 4, the Seomjin reservoir operation (scenario 3) displayed better performance in reducing the downstream flow, as shown in Figure 7a.

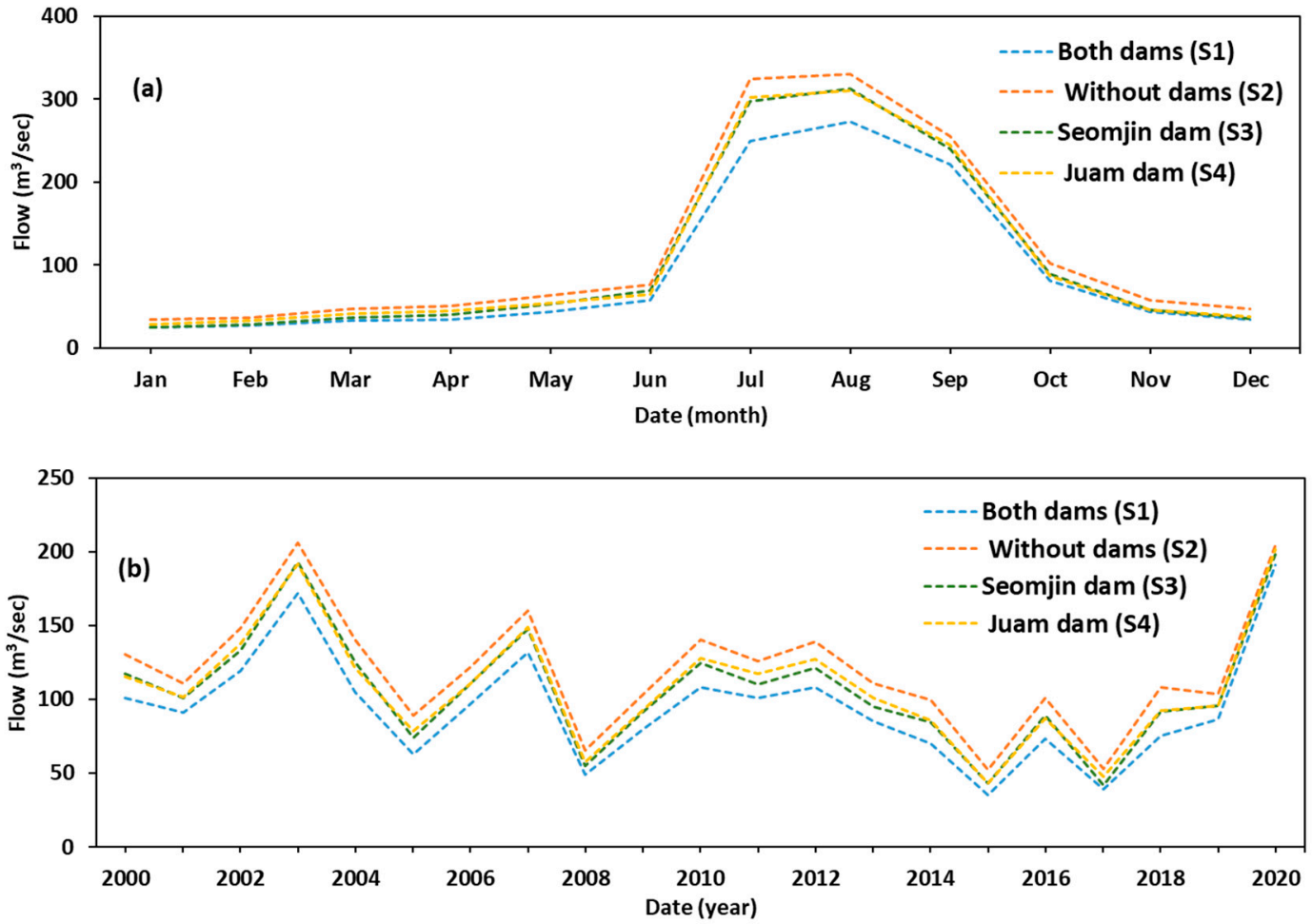

Figure 7. Reservoir operation scenario influence on the downstream flow: (**a**) monthly average and (**b**) annual average.

In the monthly hydrograph plot, the downstream flow was reduced by 75 m^3/sec when both reservoirs are operating, which occurred in July. January displayed a lower flow reduction during scenario 1 of 9.2 m^3/sec compared to scenario 2 (see Figure 7a). In the

case of scenario 3, the downstream flow reduction ranged from 6.6 to 27.4 m^3/sec for the monthly downstream hydrograph plot. Juam reservoir operation reduced the downstream flow of the basin from 3.6–22.3 m^3/sec, as displayed in Figure 7a.

Figure 7b displays the annual downstream hydrograph plots of the study basin considering the reservoir operation scenario. The year 2020 displayed the highest downstream flow values for all reservoir scenarios, except scenario 3, which occurred in 2003, as shown in Figure 7b. Similarly, the Seomjin reservoir operation displayed minimum downstream flow in 2017, while other scenarios were shown to have minimum downstream flow in 2015 (see Figure 7b). For all reservoir scenarios, the mean annual flow ranged from 94.4 to 119.7 m^3/sec for the study watershed. Simulated flow in 2006 demonstrated closer values to the mean yearly range values in all reservoir operation scenarios, as displayed in Figure 7b. For scenario 1, the maximum flow reduction occurred in 2004, with a magnitude of 35.2 m^3/sec, while lower flow decline was evident in 2020 with a value of 13.5 m^3/sec compared with scenario 2. Seomjin reservoir operation reduced the downstream flow of the study basin better than the Juam reservoir. In general, the monthly and yearly downstream flow hydrograph plots demonstrate that reservoir operations have a notable influence on reducing the streamflow of the basin, as shown in Figure 7.

Further, this study analyzed the percentage of flow reduction by comparing scenarios with no reservoir operation to those with reservoir operation in the study basin. Figure 8 illustrates the monthly and yearly percent reduction due to either one or both reservoir operations versus no reservoir operation in the study basin. Scenario 1 exhibits the highest percent flow reduction, about 32%, in April, as depicted in Figure 8a, while the lowest percent (13%) was observed in September. The month of January demonstrated a peak percentage reduction in downstream flow by 25.85%, while a lower percentage decline was observed in August of 5.4% for Seomjin reservoir operation. Scenario 4 exhibits a lower percentage (3.8%) decline in September, with the highest percentage (20.5%) noted in November. The mean monthly flow percent reduction ranges from 12.7 to 24.7% due to reservoir operation in the study basin.

Figure 8b depicts the annual flow percentage reduction due to the reservoir operation scenario in the study region. As displayed in Figure 8b, the minimum percent flow reduction occurred in 2020 for all reservoir operation scenarios. In scenario 2, the maximum percentage of flow reduction occurred in 2015, with 32.9%. In the same year, scenario 4 displayed a maximum percentage reduction of 18% in the downstream flow. In 2017, the Seomjin reservoir operation scenario displayed a peak percentage of flow reduction with a 20.15% magnitude. The average annual flow percentage reduction ranged from 9.95 to 22.6% for the reservoir operation scenarios of the study basin.

Figure 9 illustrates the monthly and yearly box plots for each reservoir operation scenario of the study watershed. The box plots specify the 25th, 50th, and 75th percentiles of the downstream flow for various scenarios, providing a comprehensive view of the flow distribution across different periods.

As displayed in Figure 9a, the simulated monthly flow box plots for each reservoir scenario in the study watershed do not include extreme values (outliers). Consequently, the maximum simulated downstream flow values for each case were within the T-shaped whisker, defined as the sum of the third quartile and 1.5 times the interquartile value. For scenario 1, the simulated maximum and minimum flow values were 273.1 and 24.7 m^3/sec, respectively. In each monthly scenario of the study basin, the third quartile range includes all simulated downstream flow values except the monsoon season (from July to September). For the scenario without a reservoir, the simulated mean monthly flow value was 119 m^3/sec, which exceeds the mean flow value by 25.15 m^3/sec of scenario 1, the lowest among all scenarios. The highest and lowest simulated monthly flow values for the case without reservoirs were 330.4 and 33.9 m^3/sec, respectively. The median value for this scenario was 61 m^3/sec, approximately half of the simulated mean monthly value. In scenarios 3 and 4, the simulated mean monthly values were 106.3 and 108.1 m^3/sec, respectively, with the median values showing a minor variation of only 0.23 m^3/sec between the

scenarios. Scenario 3 exhibited the highest and lowest downstream flow values compared to scenario 4, with the maximum value being 1.83 m^3/sec higher and the minimum value 3.37 m^3/sec lower.

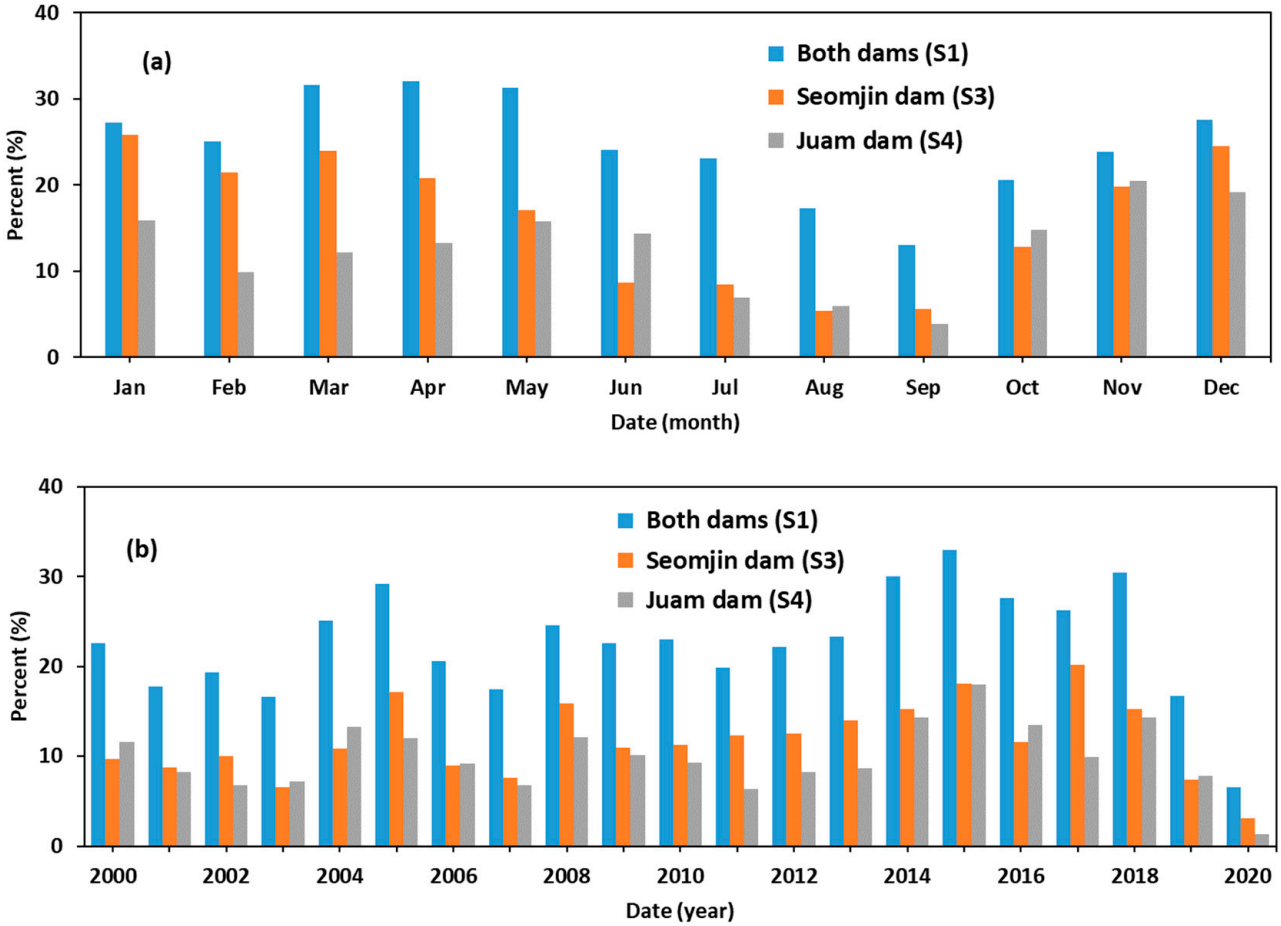

Figure 8. Percentage of flow reduction due to reservoir operation scenarios vs. non-reservoir operation: (**a**) monthly average and (**b**) annual average.

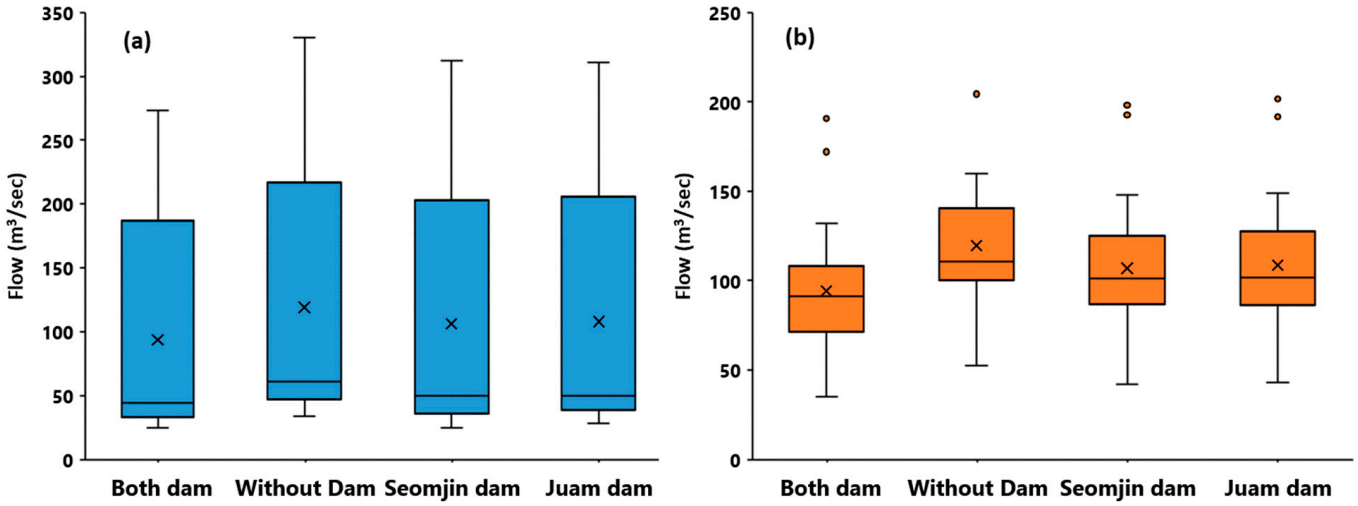

Figure 9. Box plots for reservoir operation scenarios and their downstream flow impact on the study region: (**a**) monthly average and (**b**) annual average.

In the estimated annual downstream flow box plots, multiple outliers were displayed in various scenarios, as shown in Figure 9b. For scenario 1, the simulated downstream flow of 2003 and 2020 were the maximum outliers with values of 172.1 and 190.9 m^3/sec, respectively. The mean and median flow values for scenario 1 were 94.4 and 91.1 m^3/sec, respectively. Among the simulated annual downstream flows, 52.38% of the values were inclusive in the interquartile range of scenario 1. For the natural flow scenario, the annual flows in 2003 and 2020 were beyond the maximum T-shaped whisker value at 206.3 and 204.4 m^3/sec, respectively, as illustrated in Figure 9b. The minimum downstream flow value displayed in 2015 was 52.7 m^3/sec. The mean annual downstream flow value of scenario 2 exceeded the 25.3 m^3/sec of scenario 1.

3.3. Water Balance of Seomjin River Basin

This section explores the annual basin hydrological water component values and the spatiotemporal distribution within the simulated period of the Seomjin River basin.

Table 4 presents the average annual hydrological water segment values and their contribution to the basin. Evapotranspiration (ET) accounts for the highest value (34%) of the mean annual rainfall. The high contribution of ET is due to the presence of reservoir structures in the basin that contribute to water intake from the surface area of the reservoirs. The lowest contribution for the Seomjin basin is from surface runoff, with 12.5% of the average annual precipitation. Reservoir operation and the amount of water returning to the stream could play a crucial role in the low contribution of surface runoff to the basin.

Table 4. Mean annual hydrological water balance values of Seomjin River basin from year 2000 to 2020.

	Hydrological Components					
	Precipitation	**Surface Runoff**	**Lateral Flow**	**Water Yield**	**Recharge**	**ET**
Value (mm)	1432.6	179.8	392.1	917.1	365.8	458.7
Coverage (%)		12.5	27.4	64	25.5	34

The simulated recharge amount for the basin was 365.8 mm, representing 25.5% of the regional mean annual rainfall. The water yield constituted 64% of the total Seomjin River basin mean annual rainfall amount. This value represents the total sum of the surface runoff, lateral flow, and groundwater flow of the basin within the simulated period.

Figure 10 explains the spatiotemporal distribution of the water balance constituents for the simulated period in the Seomjin River basin. The average annual ET value ranges from 386 to 592 mm, where the southwestern part of the study region showed the highest spatiotemporal value from 2000 to 2020. The northern part of the study region displayed lower values, as presented in Figure 10a. The surface runoff, with a lower contribution to the basin, ranges from 66 to 271 mm, as demonstrated in Figure 10b. The lowest average annual surface runoff occurs in subbasins 3 and 14. The maximum surface runoff occurs in subbasin 15, with 271 mm of the watershed. Subbasins 1 and 3 that enclose the reservoirs have average annual runoff values of 113 and 66 mm, respectively. The average yearly groundwater recharge of the basin ranges from 232 to 557 mm. The lowest and largest recharge occurs in subbasins 19 and 6 of the watershed. The basin elevation discrepancy plays a massive role in the groundwater recharge distribution (see Figure 1). The northern part of the Seomjin River subbasins displayed a higher recharge amount than the southern part, as displayed in Figure 10c. Water yield is an essential hydrological water component that influences the overall flow condition in the basin. The mean annual water yield ranges from 846.7 to 1008.6 mm. Subbasins 1 and 3 with reservoir operation demonstrated high water yield values of 1008.6 and 980 mm, respectively.

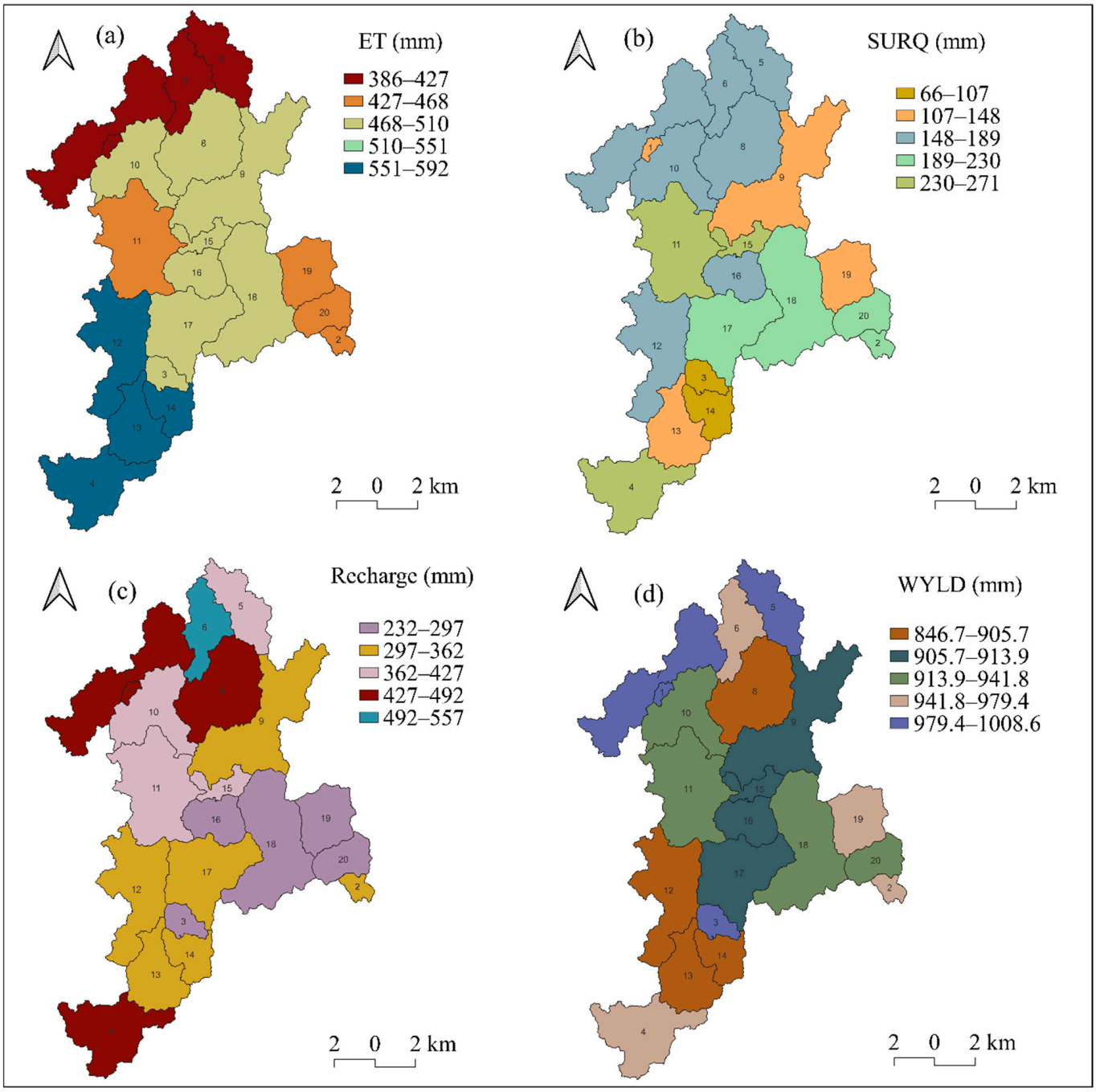

Figure 10. The study watershed hydrological water segments: (**a**) evapotranspiration (ET), (**b**) surface runoff (SURQ), (**c**) recharge, and (**d**) water yield (WYLD) in mm.

4. Discussion

Effect of Reservoir Operation on the Downstream Flow

One of the objectives of reservoir operation is to maintain optimal water storage levels following the seasonal rainfall distribution of the basin. As a result, downstream flow may fluctuate depending on the magnitude of reservoir outflows under different operational scenarios. Previous studies demonstrated that reservoir operation significantly influences the streamflow of the basin [34,45]. This study evaluates the impact of reservoir operation on the downstream flow of the Seomjin River basin through four operational scenarios, assessed on both monthly and annual scales. The present work's findings revealed that reservoir operation (scenario 1) reduced the downstream flow by up to 32% monthly and

32.9% yearly. Lee and his colleagues [34] demonstrated the effect of upstream dams on the downstream flow of the Han River basin in South Korea. They reported a similar finding, where the annual downstream flow was reduced by 31% due to upstream dam operation in the basin. Xiaobo Yun and others [46] examined the impact of reservoir operation and climate change on the streamflow in the Lancang–Mekong River basin in China. They found that reservoir operation reduced the flood risk by reducing 16% of the streamflow magnitude between 2008 and 2016. In the current study, the highest percentage reduction in the downstream flow was observed outside the monsoon season (April), with the lowest reduction occurring in September.

Further, the present study examines individual reservoir operation impacts on the downstream flow. The analysis revealed that Seomjin reservoir operation influenced the downstream flow more than Juam reservoir operation over the simulation period. In the average monthly analysis, Seomjin reservoir operation reduced the downstream flow by 3.5% more than Juam reservoir operation. However, less than 2% flow reduction variation was found in the mean annual analysis.

5. Conclusions

This research assesses the impact of multi-purpose dams on the downstream flow within the Seomjin River basin. Reservoir operation scenarios were simulated and calibrated using the SWAT model. Sensitivity analysis indicated that the calibration parameters varied according to the reservoir operation scenario. The model exhibited robust performance in calibration and validation, with R^2 and NSE values surpassing 0.75.

Peak downstream flows occurred during the monsoon season and were attributed to substantial precipitation within the basin. In scenario 1, the peak flow reduction of 32% was observed in April, whereas all scenarios demonstrated minimal reductions during the monsoon season. Monthly analyses indicated that reservoir operations led to flow reductions ranging from 3.6 m^3/s to 75 m^3/s, while annual flow reductions reached 35 m^3/s. Peak reductions were observed in 2015 for most scenarios, except for the Seomjin reservoir, which exhibited the most significant impact in 2017. When both reservoirs were operational, downstream flow reductions varied from 6.6% to 32.9% relative to the no-operation scenario. The lowest reduction in both magnitude and percentage took place in 2020.

This study further identified that the Seomjin reservoir had an ultimate influence on downstream flows in contrast to the Juam reservoir. The findings demonstrated that reservoir operations significantly altered downstream flow in the basin. Additionally, the water balance analysis showed that evapotranspiration (ET) accounted for the leading portion of the annual water budget, likely influenced by the presence of dams.

This research provides critical insights for evaluating reservoir impacts on downstream flows and provides a basis for future research, particularly regarding the impacts of reservoir operations on climate change and land-use dynamics.

Author Contributions: Conceptualization and methodology, H.H.W., S.W.C., J.E.L., and I.-M.C.; validation, H.H.W., and I.-M.C.; resources and data curation, S.W.C., J.E.L., and I.-M.C.; writing—original draft preparation, H.H.W.; writing—review and editing, H.H.W., S.W.C., J.E.L., and I.-M.C.; supervision, I.-M.C.; project administration, I.-M.C.; funding acquisition, I.-M.C. All authors have read and agreed to the published version of the manuscript.

Funding: Research for this paper was carried out under the KICT Research Program (Project No. 20240166-001, Development of IWRM-Korea Technical Convergence Platform Based on Digital New Deal) funded by the Ministry of Science and ICT.

Data Availability Statement: The original contributions presented in the study are included in the article, further inquiries can be directed to the corresponding author/s.

Conflicts of Interest: The authors declare no conflicts of interest.

References

1. Gleeson, T.; Wang-Erlandsson, L.; Porkka, M.; Zipper, S.C.; Jaramillo, F.; Gerten, D.; Fetzer, I.; Cornell, S.E.; Piemontese, L.; Gordon, L.J.; et al. Illuminating Water Cycle Modifications and Earth System Resilience in the Anthropocene. *Water Resour. Res.* **2020**, *56*, e2019WR024957. [CrossRef]
2. Falkenmark, M.; Wang-Erlandsson, L.; Rockström, J. Understanding of Water Resilience in the Anthropocene. *J. Hydrol. X* **2019**, *2*, 100009. [CrossRef]
3. Zhou, S.; Wang, Y.; Chang, J.; Su, H.; Huang, Q.; Li, Z. Quantifying the Effects of Future Environmental Changes on Water Supply and Hydropower Generation Benefits of Cascade Reservoirs in the Yellow River Basin within the Framework of Reservoir Water Supply and Demand Uncertainty. *J. Hydrol. Reg. Stud.* **2024**, *52*, 101729. [CrossRef]
4. Kim, J.; Lee, J.; Park, J.; Kim, S.; Kim, S. Improvement of Downstream Flow by Modifying SWAT Reservoir Operation Considering Irrigation Water and Environmental Flow from Agricultural Reservoirs in South Korea. *Water* **2021**, *13*, 2543. [CrossRef]
5. Wang, S.; Zhang, Z.; McVicar, T.R.; Guo, J.; Tang, Y.; Yao, A. Isolating the Impacts of Climate Change and Land Use Change on Decadal Streamflow Variation: Assessing Three Complementary Approaches. *J. Hydrol.* **2013**, *507*, 63–74. [CrossRef]
6. Zipper, S.C.; Motew, M.; Booth, E.G.; Chen, X.; Qiu, J.; Kucharik, C.J.; Carpenter, S.R.; Loheide, S.P. Continuous Separation of Land Use and Climate Effects on the Past and Future Water Balance. *J. Hydrol.* **2018**, *565*, 106–122. [CrossRef]
7. van Tol, J.; Bieger, K.; Arnold, J.G. A Hydropedological Approach to Simulate Streamflow and Soil Water Contents with SWAT+. *Hydrol. Process.* **2021**, *35*, e14242. [CrossRef]
8. Hirpa, F.A.; Alfieri, L.; Lees, T.; Peng, J.; Dyer, E.; Dadson, S.J. Streamflow Response to Climate Change in the Greater Horn of Africa. *Clim. Change* **2019**, *156*, 341–363. [CrossRef]
9. Mai, J.; Craig, J.R.; Tolson, B.A.; Arsenault, R. The Sensitivity of Simulated Streamflow to Individual Hydrologic Processes across North America. *Nat. Commun. 2022 131* **2022**, *13*, 455. [CrossRef]
10. Bourdin, D.R.; Fleming, S.W.; Stull, R.B. Streamflow Modelling: A Primer on Applications, Approaches and Challenges. *Atmosphere-Ocean* **2012**, *50*, 507–536. [CrossRef]
11. Devia, G.K.; Ganasri, B.P.; Dwarakish, G.S. A Review on Hydrological Models. *Aquat. Procedia* **2015**, *4*, 1001–1007. [CrossRef]
12. Remo, J.W.F.; Ickes, B.S.; Ryherd, J.K.; Guida, R.J.; Therrell, M.D. Assessing the Impacts of Dams and Levees on the Hydrologic Record of the Middle and Lower Mississippi River, USA. *Geomorphology* **2018**, *313*, 88–100. [CrossRef]
13. Wang, Z.; He, Y.; Li, W.; Chen, X.; Yang, P.; Bai, X. A Generalized Reservoir Module for SWAT Applications in Watersheds Regulated by Reservoirs. *J. Hydrol.* **2023**, *616*, 128770. [CrossRef]
14. López-Moreno, J.I.; Vicente-Serrano, S.M.; Beguería, S.; García-Ruiz, J.M.; Portela, M.M.; Almeida, A.B. Dam Effects on Droughts Magnitude and Duration in a Transboundary Basin: The Lower River Tagus, Spain and Portugal. *Water Resour. Res.* **2009**, *45*. [CrossRef]
15. Thomas, T.; Ghosh, N.C.; Sudheer, K.P. Optimal Reservoir Operation—A Climate Change Adaptation Strategy for Narmada Basin in Central India. *J. Hydrol.* **2021**, *598*, 126238. [CrossRef]
16. Brunner, M.I. Reservoir Regulation Affects Droughts and Floods at Local and Regional Scales. *Environ. Res. Lett.* **2021**, *16*, 124016. [CrossRef]
17. Van Loon, A.F.; Rangecroft, S.; Coxon, G.; Naranjo, J.A.B.; Van Ogtrop, F.; Van Lanen, H.A.J. Using Paired Catchments to Quantify the Human Influence on Hydrological Droughts. *Hydrol. Earth Syst. Sci.* **2019**, *23*, 1725–1739. [CrossRef]
18. Tijdeman, E.; Hannaford, J.; Stahl, K. Human Influences on Streamflow Drought Characteristics in England and Wales. *Hydrol. Earth Syst. Sci.* **2018**, *22*, 1051–1064. [CrossRef]
19. Wang, W.; Li, H.Y.; Leung, L.R.; Yigzaw, W.; Zhao, J.; Lu, H.; Deng, Z.; Demisie, Y.; Blöschl, G. Nonlinear Filtering Effects of Reservoirs on Flood Frequency Curves at the Regional Scale. *Water Resour. Res.* **2017**, *53*, 8277–8292. [CrossRef]
20. Anderson, E.P.; Jenkins, C.N.; Heilpern, S.; Maldonado-Ocampo, J.A.; Carvajal-Vallejos, F.M.; Encalada, A.C.; Rivadeneira, J.F.; Hidalgo, M.; Cañas, C.M.; Ortega, H.; et al. Fragmentation of Andes-to-Amazon Connectivity by Hydropower Dams. *Sci. Adv.* **2018**, *4*, eaao1642. [CrossRef]
21. Mumba, M.; Thompson, J.R.R. Hydrological and Ecological Impacts of Dams on the Kafue Flats Floodplain System, Southern Zambia. *Phys. Chem. Earth, Parts A/B/C* **2005**, *30*, 442–447. [CrossRef]
22. Jiao, Y.; Zhu, G.; Lu, S.; Ye, L.; Qiu, D.; Meng, G.; Wang, Q.; Li, R.; Chen, L.; Wang, Y.; et al. The Cooling Effect of Oasis Reservoir-Riparian Forest Systems in Arid Regions. *Water Resour. Res.* **2024**, *60*, e2024WR038301. [CrossRef]
23. Xing, Z.; Ma, M.; Zhang, X.; Leng, G.; Su, Z.; Lv, J.; Yu, Z.; Yi, P. Altered Drought Propagation under the Influence of Reservoir Regulation. *J. Hydrol.* **2021**, *603*, 127049. [CrossRef]
24. Lu, X.X.; Chua, S.D.X. River Discharge and Water Level Changes in the Mekong River: Droughts in an Era of Mega-Dams. *Hydrol. Process.* **2021**, *35*, e14265. [CrossRef]
25. Dash, S.S.; Sahoo, B.; Raghuwanshi, N.S. An Adaptive Multi-Objective Reservoir Operation Scheme for Improved Supply-Demand Management. *J. Hydrol.* **2022**, *615*, 128718. [CrossRef]
26. Latrubesse, E.M.; Arima, E.Y.; Dunne, T.; Park, E.; Baker, V.R.; D'Horta, F.M.; Wight, C.; Wittmann, F.; Zuanon, J.; Baker, P.A.; et al. Damming the Rivers of the Amazon Basin. *Nature* **2017**, *546*, 363–369. [CrossRef]

27. Rabelo, U.P.; Dietrich, J.; Costa, A.C.; Simshäuser, M.N.; Scholz, F.E.; Nguyen, V.T.; Lima Neto, I.E. Representing a Dense Network of Ponds and Reservoirs in a Semi-Distributed Dryland Catchment Model. *J. Hydrol.* **2021**, *603*, 127103. [CrossRef]
28. Firoz, A.B.M.; Nauditt, A.; Fink, M.; Ribbe, L. Quantifying Human Impacts on Hydrological Drought Using a Combined Modelling Approach in a Tropical River Basin in Central Vietnam. *Hydrol. Earth Syst. Sci.* **2018**, *22*, 547–565. [CrossRef]
29. Nguyen, B.Q.; Kantoush, S.A.; Saber, M.; Van Binh, D.; Vo, N.D.; Sumi, T. Quantifying the Impacts of Hydraulic Infrastructure on Tropical Streamflows. *Hydrol. Process.* **2023**, *37*, e14834. [CrossRef]
30. Qiu, H.; Qi, J.; Lee, S.; Moglen, G.E.; McCarty, G.W.; Chen, M.; Zhang, X. Effects of Temporal Resolution of River Routing on Hydrologic Modeling and Aquatic Ecosystem Health Assessment with the SWAT Model. *Environ. Model. Softw.* **2021**, *146*, 105232. [CrossRef]
31. Zajac, Z.; Revilla-Romero, B.; Salamon, P.; Burek, P.; Hirpa, F.; Beck, H. The Impact of Lake and Reservoir Parameterization on Global Streamflow Simulation. *J. Hydrol.* **2017**, *548*, 552–568. [CrossRef] [PubMed]
32. Dynesius, M.; Nilsson, C. Fragmentation and Flow Regulation of River Systems in the Northern Third of the World. *Science* **1994**, *266*, 753–762. [CrossRef] [PubMed]
33. Abbott, B.W.; Bishop, K.; Zarnetske, J.P.; Minaudo, C.; Chapin, F.S.; Krause, S.; Hannah, D.M.; Conner, L.; Ellison, D.; Godsey, S.E.; et al. Human Domination of the Global Water Cycle Absent from Depictions and Perceptions. *Nat. Geosci.* **2019**, *12*, 533–540. [CrossRef]
34. Lee, J.E.; Heo, J.H.; Lee, J.; Kim, N.W. Assessment of Flood Frequency Alteration by Dam Construction via SWAT Simulation. *Water* **2017**, *9*, 264. [CrossRef]
35. Zhou, C.; Sun, N.; Chen, L.; Ding, Y.; Zhou, J.; Zha, G.; Luo, G.; Dai, L.; Yang, X. Optimal Operation of Cascade Reservoirs for Flood Control of Multiple Areas Downstream: A Case Study in the Upper Yangtze River Basin. *Water* **2018**, *10*, 1250. [CrossRef]
36. Donchyts, G.; Winsemius, H.; Baart, F.; Dahm, R.; Schellekens, J.; Gorelick, N.; Iceland, C.; Schmeier, S. High-Resolution Surface Water Dynamics in Earth's Small and Medium-Sized Reservoirs. *Sci. Rep.* **2022**, *12*, 13776. [CrossRef]
37. Arheimer, B.; Donnelly, C.; Lindström, G. Regulation of Snow-Fed Rivers Affects Flow Regimes More than Climate Change. *Nat. Commun.* **2017**, *8*, 62. [CrossRef]
38. Yang, Y.; Roderick, M.L.; Yang, D.; Wang, Z.; Ruan, F.; McVicar, T.R.; Zhang, S.; Beck, H.E. Streamflow Stationarity in a Changing World. *Environ. Res. Lett.* **2021**, *16*, 064096. [CrossRef]
39. Kim, H.; Parajuli, P.B. Impacts of Reservoir Outflow Estimation Methods in SWAT Model Calibration. *Trans. ASABE* **2014**, *57*, 1029–1042. [CrossRef]
40. Arnold, J.G.; Srinivasan, R.; Muttiah, R.S.; Williams, J.R. Large Area Hydrologic Modeling and Assessment Part I: Model Development. *J. Am. Water Resour. Assoc.* **1998**, *34*, 73–89. [CrossRef]
41. Neitsch, S.L.; Arnold, J.G.; Kiniry, J.R.; Williams, J.R. *Soil and Water Assessment Tool Theoretical Documentation Version 2009*; Texas Water Resources Institute: College Station, TX, USA, 2011.
42. Moriasi, D.N.; Arnold, J.G.; Van Liew, M.W.; Bingner, R.L.; Harmel, R.D.; Veith, T.L. Model Evaluation Guidelines for Systematic Quantification of Accuracy in Watershed Simulations. *Trans. ASABE* **2007**, *50*, 885–900. [CrossRef]
43. Wannasin, C.; Brauer, C.C.; Uijlenhoet, R.; van Verseveld, W.J.; Weerts, A.H. Daily Flow Simulation in Thailand Part II: Unraveling Effects of Reservoir Operation. *J. Hydrol. Reg. Stud.* **2021**, *34*, 100792. [CrossRef]
44. Li, D.; Long, D.; Zhao, J.; Lu, H.; Hong, Y. Observed Changes in Flow Regimes in the Mekong River Basin. *J. Hydrol.* **2017**, *551*, 217–232. [CrossRef]
45. Tian, J.; Chang, J.; Zhang, Z.; Wang, Y.; Wu, Y.; Jiang, T. Influence of Three Gorges Dam on Downstream Low Flow. *Water* **2019**, *11*, 65. [CrossRef]
46. Yun, X.; Tang, Q.; Wang, J.; Liu, X.; Zhang, Y.; Lu, H.; Wang, Y.; Zhang, L.; Chen, D. Impacts of Climate Change and Reservoir Operation on Streamflow and Flood Characteristics in the Lancang-Mekong River Basin. *J. Hydrol.* **2020**, *590*, 125472. [CrossRef]